Earthquake Geotechnical Engineering for Protection and Development of Environment and Constructions – Silvestri & Moraci (Eds)
© 2019 Associazione Geotecnica Italiana, Rome, Italy, ISBN 978-0-367-14328-2

The effect of soil-structure interaction and liquefaction on the seismic performance of typical port buildings

S. Karafagka, S. Fotopoulou, A. Karatzetzou & D. Pitilakis
Aristotle University, Thessaloniki, Greece

ABSTRACT: Although progress has been made on the influence of soil liquefaction and soil-structure interaction (SSI) on the structural response, studies combining both phenomena are very limited, if not existent. To bridge this gap, the objective of this study is to implement a numerical investigation of the influence of both liquefaction and SSI on the seismic performance of typical reinforced concrete (RC), low-code (LC), moment resisting frame (MRF) port buildings. In particular, the following numerical modelling approaches are applied: i) a fixed-base structural model subjected to free-field motion that neglects liquefaction and SSI; ii) a fixed-base structural model subjected to free-field motion that considers liquefaction; iii) a SSI system that neglects liquefaction; iv) a SSI system that considers liquefaction. Finally, comparative results of the above numerical approaches are presented, which show the significant role of liquefaction and SSI in altering the expected structural performance of port buildings.

1 INTRODUCTION

Severe physical damages to port facilities during past seismic events led to important economic and societal losses as seen recently after the earthquakes in Kocaeli (Turkey) 1999; Christchurch (New Zealand) 2011 and Emilia-Romagna (Northern Italy) 2012. The most common source of seismic damage to port infrastructure is the liquefaction of loose, saturated soils that often prevail at coastal areas (Pitilakis et al. 2014). In addition, soil-structure interaction (SSI) may also play a significant role on the seismic performance of port structures, modifying their dynamic characteristics, as well as the seismic response at foundation level.

Traditionally, the seismic behaviour of structures is estimated assuming fixed-base conditions, which may be a reasonable hypothesis only for structures founded on rock or very stiff soil. Nevertheless, the seismic response of a structure resting on deformable soil may differ significantly compared to the fixed-base assumption (Mylonakis and Gazetas 2000). There are two main approaches that are commonly used for the analysis of the SSI phenomenon: the "direct approach", where soil, foundation and structure are modelled and analysed as a single system, and the "substructure approach", where SSI is analysed as two separate systems where the coupling of the interacting subdomains is achieved using impedance functions. The incorporation of SSI phenomena in the analysis has been generally believed to be beneficial, as SSI effects generally tend to reduce force demands on the structure. However, in nonlinear soil-structure systems additional translation and rotation effects may be produced during strong shaking increasing the displacement demands of the structure (Karapetrou et al. 2015). The problem is expected to be even more complicated when soil liquefaction phenomena are present. However, numerical modelling techniques for estimating the influence of both soil liquefaction and SSI effects on the structural response, has not received much attention and hence requires further investigation.

This study aims at examining the contribution of liquefaction and SSI on the seismic performance of typical RC, low-code, MRF port buildings. The numerical modelling approaches used for the investigation are a fixed-base structural model subjected to free-field motion that neglects liquefaction and SSI, a fixed-base structural model subjected to free-field motion that considers liquefaction, a SSI system that neglects liquefaction, as well as a SSI system that considers liquefaction. Comparative results are presented, in terms of Arias intensity and acceleration time histories at the structure foundation as well as drift demands on the structure.

2 NUMERICAL MODELLING

2.1 *Selection of the structural typology*

A two-storey three-bay MRF RC building representative of Thessaloniki port critical buildings is selected as reference structure (Kappos et al. 2006) for the investigation. It has been designed with a low seismic code according to the 1959 Greek seismic regulations ('Royal Decree' of 1959) in which the ductility and the dynamic features of the structures are completely neglected. The height of the 1^{st} storey is 4.5m and that of the upper storeys is 3.0m. Figure 1 illustrates a schematic view of the reference building model, whereas Table 1 presents its main characteristics, namely the total mass, the fundamental period and the strength of concrete and steel.

2.2 *Structural modelling*

Two-dimensional numerical simulation of the selected building typology is conducted using the OpenSees finite element platform (Mazzoni et al. 2009). Inelastic force-based formulations are implemented for the nonlinear beam-column frame element modelling. Distributed material inelasticity is applied based on the fibre approach to represent the cross-sectional behaviour. In the present analysis, for the concrete the uniaxial "Concrete01" material is used to construct a uniaxial Kent-Scott-Park (Scott et al. 1982) concrete material object with degraded linear unloading/reloading stiffness according to the work of Karsan-Jirsa (Karsan and Jirsa 1969) and zero tensile strength. Different material parameters are adopted for the confined (core) and the unconfined (cover) concrete. For the steel reinforcement, the uniaxial "Steel01" material is used to construct a uniaxial bilinear steel material object with kinematic hardening described by a non-linear evolution equation. Finally, full bond is assumed between the foundation and the soil nodes.

2.3 *Soil–structure interaction modelling*

One representative soil profile of the port area of Thessaloniki simplified regarding its total depth, with fundamental period T_o theoretically estimated equal to 0.73sec, is considered to

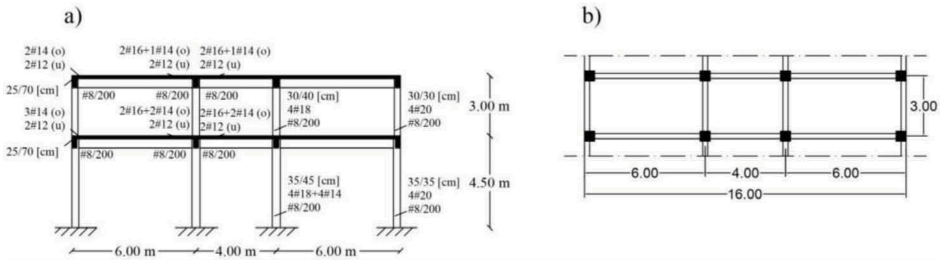

Figure 1. Schematic representation of the (a) cross-section with reinforcement details and (b) plan view of the reference MRF building used for the study (personal communication Kappos A and Panagopoulos G).

Table 1. Main characteristics of the reference building typology.

Total mass (tn)	Fundamental period T(sec)	f_c (MPa)	f_y (MPa)
65.7	0.43	14.0	400.0

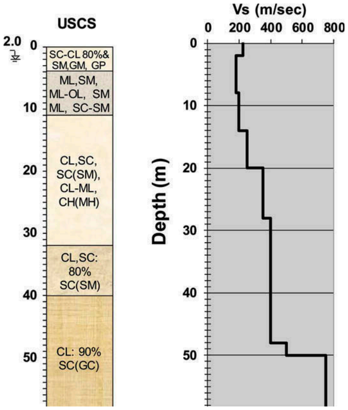

Figure 2. Schematic representation of the layered soil profile together with a general geotechnical characterization according to USCS classification as well as Vs profile.

compute the ground response. The liquefaction potential of the subsoil layers of the selected soil profile was quantitatively evaluated by taking into account the guidelines of EC8 as well as the collected geotechnical information of the port area and the available SPT and laboratory data (Pitilakis et al. 2018). Liquefiable soil formations were found at depths three to fourteen meters, which are basically silty/clayey sands and nonplastic silts with low values of N_{SPT}. Thus, knowing that the liquefaction susceptibility in the port area is rather high, this soil profile refers to ground type S according to EC8 classification. Figure 2 presents a schematic representation of the adopted layered soil profile together with a general geotechnical characterization according to USCS classification as well as the V_s profile.

Two-dimensional (2D) dynamic analyses of the SSI models are conducted with OpenSees. The grid adopted for the soil has a depth equal to 50m with total length of 150m to avoid spurious wave reflections at the vertical boundaries. A relatively dense discretization with quadrilateral elements of 0.5m x 2.0m is adopted, considering that the maximum frequency of interest is set to 10Hz. This mesh allows an adequate number of elements to fit within the shortest wavelength of the propagating shear wave.

The entire soil profile is underlain by an elastic half-space which represents the finite rigidity of the underlying bedrock. The groundwater table is located at 2.0m depth, therefore, saturated unit weights are used for the soil below this level and effective stress analysis is considered through the use of nine-node quadrilateral elements with both displacement and pore pressure degrees of freedom. Such elements are able to simulate fluid-solid coupling during the earthquake excitation, based on Biot's theory of porous medium (Biot 1962). In particular, the corner nodes of a nine-node element have three degrees of freedom, two translational and one pore pressure, while the interior nodes have only two translational degrees of freedom. A Lysmer-Kuhlemeyer (1969) dashpot is utilized to account for the finite rigidity of the underlying half-space using a bedrock shear wave velocity of 750m/s and mass density of 2.2Mg/m^3. To model the underlying elastic half-space necessitates that the nodes at the base of the soil model be left free to displace in the horizontal direction, be all given the same horizontal displacements and finally be fixed against vertical translation only. Periodic boundary conditions are used to ensure that free-field conditions exist at the horizontal boundaries of the model. In particular, the displacement degrees of freedom for the nodes on either side of the soil model are tied together imposing the same translational displacements in x and z directions, and rotation about the y-axis.

A fully coupled (u-P) formulation is employed which is capable of simulating permanent shear-strain accumulation in clean medium-dense cohesionless soils during liquefaction and dilation due to increased cyclic shear stiffness and strength. The soil constitutive behaviour is based on the framework of multi-surface (nested-surface) plasticity (Prevost 1985), with modifications by Yang (2000). The hardening law, the yield surface and the flow rule constitute the major components of the plasticity model. During the application of gravity load, material behaviour is linear elastic. In the subsequent dynamic loading phase, the stress-strain response is elastic-plastic. A purely deviatoric kinematic hardening rule (Prevost 1985) is employed in order to generate soil hysteretic response under cyclic loading. This kinematic rule dictates that all yield surfaces may translate in stress space within the failure envelope (Parra 1996; Yang 2000) and is consistent with the Masing unloading/reloading criteria (Masing 1926). For the cohesionless soil layers, an elastic-plastic material, namely "PressureDependMultiYield02", is used in Opensees, where the yield function is assumed to follow the Drucker-Prager shape. The Drucker-Prager yield surface is described in effective stress space as a function of friction angle and cohesion (as defined in the Mohr-Coulomb failure criteria). Plasticity is formulated based on the multi-surface concept, with a non-associative flow rule (Parra 1996) that handles the soil contractive/dilative behaviour during shear loading to achieve appropriate interaction between shear and volumetric responses. For the cohesive soil layers, an elastic-plastic material in which plasticity exhibits only in the deviatoric stress-strain response, namely "PressureIndependMultiYield", is used. The volumetric stress-strain response is linear-elastic and is independent of the deviatoric response. This material is implemented to simulate monotonic or cyclic response of materials whose shear behaviour is insensitive to the confinement change. The yield function is assumed to follow the Von Mises shape. The Von Mises yield surface is a function solely of undrained shear strength. Plasticity is formulated based on the multi-surface concept, with an associative flow rule in which the incremental plastic strain vector is normal to the yield surface.

2.4 *Effect of SSI and liquefaction*

Four modelling approaches are applied to investigate the importance of SSI and liquefaction effects on the seismic performance of typical low-code MRF RC port buildings. 1) In the first one, a fixed-base structural model subjected to free-field motion that neglects liquefaction and SSI is considered. The free-field ground shaking motion results from a non-linear 1D seismic response analysis of the selected typical soil profile. This free-field motion, is imposed as input ground motion to the fixed-base structural model to compute its response. This fixed-base approach is used as a reference and benchmark to highlight the significant effects of SSI and liquefaction on the structural performance. 2) The second approach includes a fixed-base structural model subjected to free-field motion that considers liquefaction. This two-step uncoupled approach considers the liquefaction effects on the free-field response using an appropriate constitutive model for the examined soil profile. The free-field response is then applied to the fixed-base structure neglecting, thus, the SSI effects. 3) In the third approach, a SSI system that neglects liquefaction is considered. A direct one-step approach where the soil, the foundation and the structure are modelled and analysed as a single system is used neglecting soil liquefaction on the structural response. 4) In the final approach, a SSI system that considers liquefaction is studied. SSI is modelled by applying again the direct one-step approach considering soil nonlinearity, introduced by soil liquefaction.

3 SEISMIC INPUT MOTION

A set of 15 accelerograms (Table 2) is selected from the European Strong-Motion Database to perform the analyses. They are all referring to rock type or stiff soils (ground types A and B according to EC8) with moment magnitude (M_w) and epicentral distance R that range between $5.5<M_w<6.5$ and $0<R<45$km respectively. The primary selection criterion is the average acceleration spectra of the set to be of minimal "epsilon" (Baker and Cornell 2005) at the period range of $0.00<T<2.00$sec with respect to the corresponding 5% damped median plus 0.5 standard deviations spectrum defined based on the ground motion prediction equation (GMPE) proposed by Akkar and Bommer (2010). The optimization procedure is performed using REXEL software (Iervolino et al. 2010) that allows obtaining combinations of accelerograms, which on average are compatible to the reference spectrum.

Table 2. List of earthquake records used for the dynamic analyses.

Earthquake Name	Date	Mw	Fault Mechanism	Epicentral Distance [km]	PGA [m/s^2]	EC8 Site class	Waveform ID
Umbria Marche (aftershock)	10/6/1997	5.5	normal	5	1.838	A	651
Valnerina	9/19/1979	5.8	normal	5	1.510	A	242
SE of Tirana	1/9/1988	5.9	thrust	7	4.037	A	3802
Lazio Abruzzo (aftershock)	5/11/1984	5.5	normal	15	1.411	A	990
Valnerina	9/19/1979	5.8	normal	5	2.012	A	242
Kozani	5/13/1995	6.5	normal	17	2.039	A	6115
Friuli (aftershock)	9/15/1976	6	thrust	12	1.339	A	149
Umbria Marche	9/26/1997	5.7	normal	23	1.645	A	763
Friuli (aftershock)	9/15/1976	6	thrust	14	2.586	B	134
Patras	7/14/1993	5.6	strike slip	9	3.337	B	1932
Kalamata	9/13/1986	5.9	normal	11	2.670	B	414
Umbria Marche 2	9/26/1997	6	normal	11	5.138	B	594
Montenegro (aftershock)	5/24/1979	6.2	thrust	17	1.708	B	229
Kefallinia island	1/23/1992	5.6	thrust	14	2.223	B	6040
Ano Liosia	9/7/1999	6	normal	14	2.159	B	1714

4 COMPARATIVE DYNAMIC ANALYSIS

The significant role of SSI and liquefaction on the seismic response of typical low-code MRF RC port buildings is illustrated below, conducting comparative analyses for the different considered modelling approaches. More specifically, dynamic analyses are conducted using the earthquake records of Table 2 as input motions at the bedrock, all scaled to a peak ground acceleration (PGA) level equal to 0.3g. It should be noted that although the soil profile described above is liquefiable, in the two modelling approaches liquefaction potential is not considered. This was achieved by setting the constants defining the pore pressure build-up of the liquefiable layers equal to zero. This fact is demonstrated in Figure 3, which shows the computed variation of effective confinement with depth and stress-strain hysteretic loops at specific depth for the representative soil profile where liquefaction is taken (Figure 3, bottom) and is not taken (Figure 3, top) into account. In particular, layers of potential liquefaction may be identified by the loss of effective confining stress (equal to zero) which is also verified by the corresponding stress-strain loops (e.g. at 7.0m below surface).

The results of the dynamic analyses are obtained in terms of acceleration time histories at the base of the structure, Arias intensity (I_A) and the maximum interstorey drift ratio (maxISD) for the different analysed configurations. Figure 4 displays PGA - maxISD and I_A - maxISD pairs for the SSI and fixed-base models considering or not liquefaction. It is noted that the acceleration time histories imposed at the four footings of the structure are not the same, thus the maximum PGA imposed at the foundation level is considered. Generally, it is seen that the ground motion characteristics (frequency content and duration) play a significant role to the structural response in terms of maxISD as witnessed by the large scatter in the computed maxISD. It is shown that the seismic intensity in terms of PGA and I_A at the base of the structure is greater in the cases where liquefaction is not taken into account with the SSI cases generally shown higher values. This could be attributed to the fact that when liquefaction occurs the seismic energy is further dissipated in the soil due to the pore pressure increase. Although the seismic intensity is decreased in the cases where liquefaction is taken into account, the corresponding drift demand values are comparable with the ones of the non-liquefiable cases. Thus, especially in the cases where liquefaction is taken into account, neither PGA nor I_A is a good metric of the seismic intensity as they do not have a good correlation with drift demand and they cannot fully describe the seismic ground motion due to the increased nonlinearity introduced by the soil liquefaction. Thus, the knowledge of a second IM (i.e. the permanent absolute or differential ground displacements at the structure foundation level), especially for liquefiable soils where liquefaction displacements are also imposed

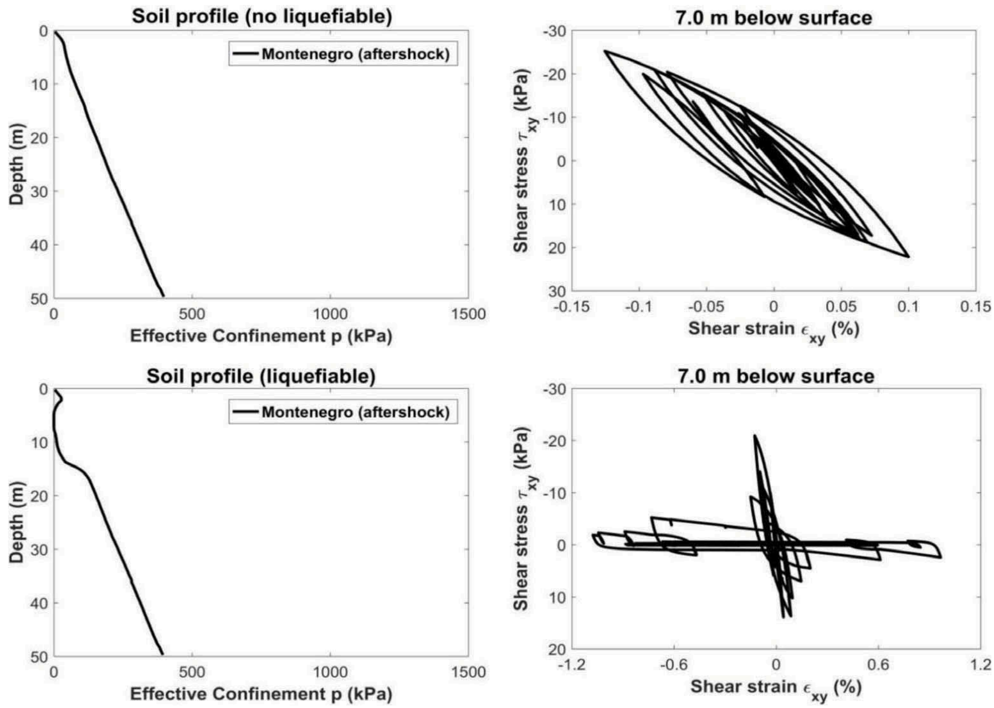

Figure 3. Variation of the effective confinement with depth and stress-strain hysteretic loops at 7.0m depth for the ID 229 input motion for the liquefiable (bottom) and the non-liquefiable (top) cases.

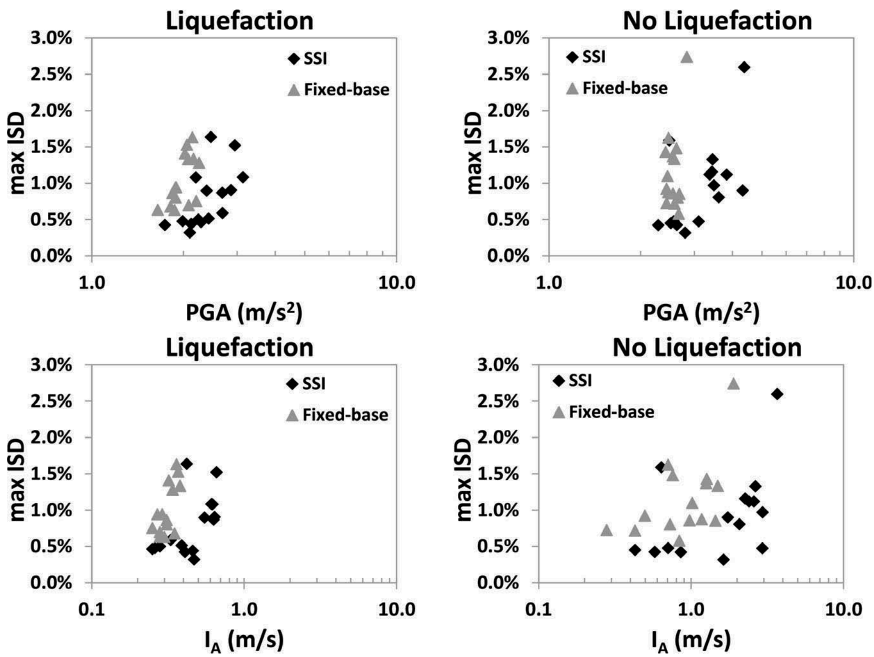

Figure 4. PGA - maxISD and I_A - maxISD pairs for the SSI and fixed-base models considering or not liquefaction.

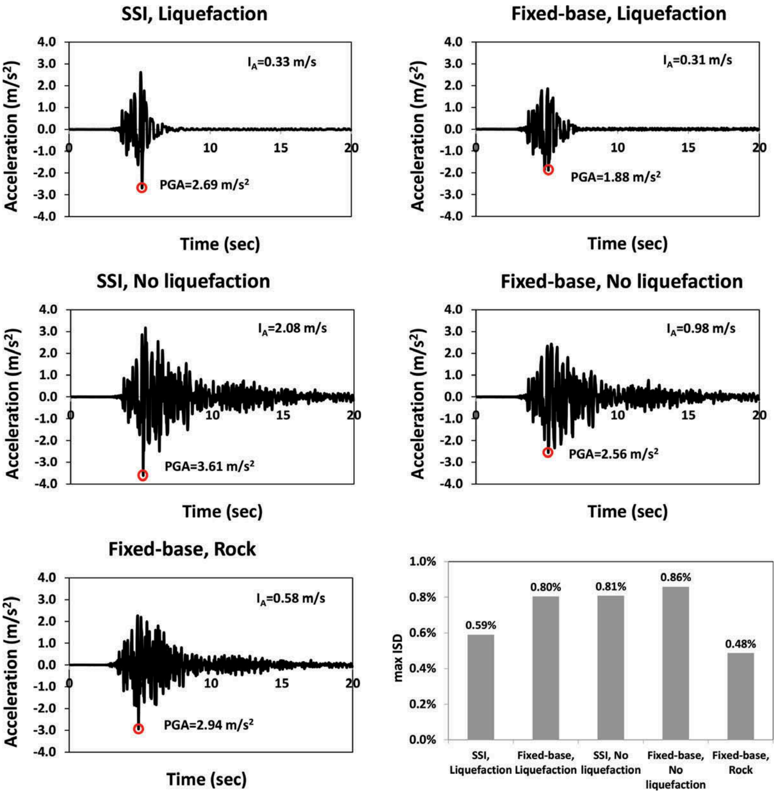

Figure 5. Acceleration time histories at the base of the structure and maxISD ratio for the different analysed configurations for Umbria Marche aftershock (ID 651) input motion at rock scaled to a PGA = 0.3g.

to the structure foundation, should be also taken into account, as they may provide valuable information for the seismic response assessment of buildings.

Indicatively, the results of the dynamic analyses conducted using Umbria Marche record (ID 651) as rock input motion scaled to a PGA equal to 0.3g, are presented in Figure 5 for the different analysed configurations. The highest maxISD is shown for the fixed-base structural configuration, which does not consider soil liquefaction, whereas the lowest one is presented for the fixed-base model where the building receives directly the rock input motion. This trend is observed at most of the cases, however there are a few cases where the lowest maxISD is seen for the SSI system which considers liquefaction.

5 CONCLUSIONS

Comparative dynamic results were conducted for the fixed-base models and the soil-structure systems (considering or not liquefaction) for a selected set of earthquake records to demonstrate the influence of SSI and liquefaction on the seismic performance of buildings. Results in terms of Arias intensity, acceleration time histories at the base of the structure and drift demands on the structure, as well as effective confinement profiles and stress-strain hysteretic loops at specific soil depths highlighted the significant role of SSI and liquefaction in modifying the ground motion imposed at the base of the structure and finally its structural dynamic response. The level of this modification depends on the ground motion characteristics (frequency content and duration). In general, especially for liquefiable soils where increased soil nonlinearity is introduced, neither PGA nor I_A on their own can adequately describe the seismic response and therefore an additional IM (i.e. the Permanent Ground Displacements or differential displacements at the foundation level of the structure) should be taken into account. The combined knowledge of these two IMs may provide valuable information for the seismic response assessment of buildings subjected to the combined ground shaking and liquefaction.

ACKNOWLEDGMENTS

This study was carried out in the framework of the "Resilient, system-wide seismic risk assessment of port facilities. Application to Thessaloniki Port system" RESPORTS project (http://resports.gr/), funded by the Hellenic Foundation for Research and Innovation (HFRI) and General Secretariat for Research and Technology (GSRT) under Grant Agreement Number 754. In addition, the first author would like to acknowledge the support by the project "Innovative system for monitoring and early warning of schools and infrastructure against earthquakes and other hazards - SAFESCHOOLS" (MIS5030314) which is funded by the Operational Programme "Competitiveness, Entrepreneurship and Innovation" (NSRF 2014-2020) and co-financed by Greece and the European Union (European Regional Development Fund).

REFERENCES

Akkar, S. & Bommer, J.J. 2010. Empirical equations for the prediction of PGA, PGV and spectral accelerations in Europe, the Mediterranean and the Middle East. *Seismol Res Lett*, 81:195–206.

Baker, J.W. & Cornell, C.A. 2005. A vector valued ground motion intensity measure consisting of spectral acceleration and epsilon. *Earthq Eng Struct D*, 34:1193–1217.

Biot, M.A. 1962. Mechanics of deformation and acoustic propagation in porous media. *J Appl Phys*, 33 (4):1482–1498.

Iervolino, I., Galasso, C., Cosenza, E. 2010. REXEL:computer aided record selection for code-based seismic structural analysis. *Bull Earthq Eng*, 8:339–362.

Kappos, A.J., Panagopoulos, G., Panagiotopoulos, C., Penelis, G. 2006. A hybrid method for the vulnerability assessment of R/C and URM buildings. *Bull Earthq Eng*, 4:391–419.

Karapetrou, S., Fotopoulou, S., Pitilakis, K. 2015. Seismic vulnerability assessment of high-rise non-ductile RC buildings considering soil–structure interaction effects, *Soil Dyn Earthq Eng*, 73: 42–57.

Karsan, I. & Jirsa, J. 1969. Behavior of concrete under compressive loading. *J Struct Div*, ASCE, 95:2543–2563.

Lysmer, J. & Kuhlemeyer, A.M. 1969. Finite dynamic model for infinite media. *J Eng Mech Div*, ASCE, 95:859–877.

Masing, G. 1926. Eigenspannungen and verfertigung beim messing. *Proc. 2nd Int. Congress on Applied Mech.*, Zurich, Switzerland.

Mazzoni, S., McKenna, F., Scott, M.H., Fenves, G.L. 2009. Open system for earthquake engineering simulation user command-language manual. University of California, Berkeley: Pacific Earthquake Engineering Research Center.

Mylonakis, G. & Gazetas, G. 2000. Seismic soil-structure interaction: beneficial or detrimental. *J Earthq Eng*, 4(3):277–301.

Parra, E. 1996. *Numerical modelling of liquefaction and lateral ground deformation including cyclic mobility and dilation response in soil systems*. Ph.D.thesis. Troy, NY: Department of Civil Engineering, Rensselaer Polytechnic Institute.

Pitilakis, K., Crowley, H., Kaynia, A. (Eds) 2014. SYNER-G: Typology definition and fragility functions for physical elements at seismic risk. Buildings, lifelines, transportation networks and critical facilities. *Geotechnical, Geological and Earthquake Engineering*, 27, Springer, The Netherland.

Pitilakis, K., Argyroudis, S., Fotopoulou, S., Karafagka, S., Kakderi, K., Selva, J. 2018. Application of stress test concepts for port infrastructures against natural hazards. The case of Thessaloniki port in Greece. *Reliability Engineering & System Safety*, https://doi.org/10.1016/j.ress.2018.07.005.

Prévost, J.H. 1985. A simple plasticity theory for frictional cohesionless soils. *Soil Dyn Earthq Eng*, 4:9–17.

Scott, B.D., Park, R., Priestley, M.J.N. 1982. Stress-strain behavior of concrete confined by overlapping hoops at low and high strain rates. *Journal of the American Concrete Institute*, 79(1):13–27.

Yang, Z. 2000. *Numerical modelling of earthquake site response including dilation and liquefaction*. Ph.D. thesis. New York: Dept. of Civil Engineering and Engineering Mechanics, ColumbiaUniversity.